

Fermi surface of the Pr-based filled skutterudite compound PrOs₄P₁₂

H. Sugawara, Y. Iwahashi, K. Magishi, T. Saito, and K. Koyama

Faculty of the Integrated Arts and Sciences, The University of Tokushima, Tokushima 770-8502, Japan

H. Harima

Department of Physics, Kobe University, Kobe 657-8501, Japan

D. Kikuchi and H. Sato

Department of Physics, Tokyo Metropolitan University, Minami-Ohsawa, Hachioji, Tokyo 192-0397, Japan

T. Endo, R. Settai, and Y. Ōnuki

Graduate School of Science, Osaka University, Toyonaka, Osaka 560-0043, Japan

(Received 16 September 2008; revised manuscript received 1 December 2008; published 7 January 2009)

We have investigated the Fermi-surface (FS) properties in the Pr-based filled skutterudite PrOs₄P₁₂ and its reference compound LaOs₄P₁₂ by means of de Haas–van Alphen experiments and the band-structure calculations. The topology of FS in PrOs₄P₁₂ is close to that in the reference compound LaOs₄P₁₂, indicating a localized nature of 4*f* electrons in PrOs₄P₁₂. Whereas the localized nature of 4*f* electrons, we have confirmed a highly enhanced cyclotron effective mass of up to 18*m*₀ in PrOs₄P₁₂, which is enhanced about 3.8 times compared to that in LaOs₄P₁₂. No nesting property with $q=(1,0,0)$ in the FS of PrOs₄P₁₂ has been confirmed in contrast to good nesting properties in PrFe₄P₁₂ and PrRu₄P₁₂ which exhibit unusual ordered states at low temperatures. A role of both the 4*f* electron's contributions and the FS nesting property for unusual phase transitions are discussed.

DOI: [10.1103/PhysRevB.79.035104](https://doi.org/10.1103/PhysRevB.79.035104)

PACS number(s): 71.18.+y, 71.27.+a

I. INTRODUCTION

The filled skutterudite compounds RT_4X_{12} (R =rare earth; T =Fe, Ru, and Os; and X =pnictogen) have attracted much attention because of the novel physical properties, i.e., heavy-fermion (HF) state, metal-insulator (M-I) transition, anisotropic superconductivity, etc.^{1–3} Pr-based skutterudites are particularly interesting in which a hybridization and multipole interaction of 4*f* electrons are believed to play an important role for the anomalous properties. Among them, both PrFe₄P₁₂ and PrRu₄P₁₂ exhibit unusual nonmagnetic ordered states below $T_A=6.5$ K for the former and $T_{MI}=63$ K for the latter in zero field.^{4–8} In the former, the HF behavior appears when the low-field-ordered state is suppressed by magnetic fields.^{5–7} From the band-structure calculations, Harima and co-workers^{9–11} suggested that these transitions could be triggered by the nearly perfect nesting of those main Fermi surfaces (FSs) with $q=(1,0,0)$; these main FSs are reconstructed due to those instabilities involving the crystal distortion from body-centered-cubic (bcc) to simple cubic (sc) structure. However, both LaFe₄P₁₂ and LaRu₄P₁₂ without 4*f* electrons having basically the same FSs as those in the Pr-based homologs show a superconducting transition at 4.6 and 7 K, respectively, without any other phase transition. These facts suggest the 4*f* electrons' contribution promoting the FS nesting effect on these unusual transitions beyond the simple FS nesting scenario. Recently, a role of multipole interaction of 4*f* electrons correlated with the good nesting properties is suggested for these phase transitions from theoretical point of view.¹² In order to clarify the origin of the unusual ordered states, it is crucial to investigate the physical properties of the sister compound PrOs₄P₁₂ that does not show any anomaly down to 50 mK.^{8,13–15}

The first measurements of the temperature T dependences of magnetic susceptibility $\chi(T)$ and specific heat $C(T)$ in PrOs₄P₁₂ have been reported on the polycrystalline samples synthesized by the high-pressure technique.^{8,13} $\chi(T)$ shows a Curie-Weiss behavior with the effective magnetic moment of $3.63\mu_B$, which is close to $3.58\mu_B$ for Pr³⁺, and paramagnetic Weiss temperature of -17 K indicating antiferromagnetic correlation.⁸ Sommerfeld coefficient in PrOs₄P₁₂ was reported to be 56.5 mJ/K² mol which is 2.6 times larger than 21.6 mJ/K² mol in reference material LaOs₄P₁₂.¹³ On the other hand, from the recent studies on single-crystalline samples in PrOs₄P₁₂,¹⁴ such a mass enhancement is still controversial, where the Sommerfeld coefficient has been estimated to be 26 mJ/K² mol, indicating more than a factor 2 different from that reported on polycrystalline sample. The Sommerfeld coefficient on single-crystalline sample of LaOs₄P₁₂ has not yet been reported since it may be difficult to grow the large single crystal for $C(T)$ measurements. It is crucial to compare directly the effective mass between these compounds using high quality single crystals to settle the mass enhancement in PrOs₄P₁₂. The de Haas–van Alphen (dHvA) effect is the most powerful tool to investigate the electronic state such as FS and effective mass. In this paper, we report the successful dHvA effect both in LaOs₄P₁₂ and PrOs₄P₁₂. The experimental result is compared with the band-structure calculation based on a full potential linearized augmented-plane-wave (FLAPW) method within the local-density approximation (LDA).

II. EXPERIMENTAL METHODS

Single crystals of LaOs₄P₁₂ and PrOs₄P₁₂ were grown by the tin-flux method which is basically the same as described

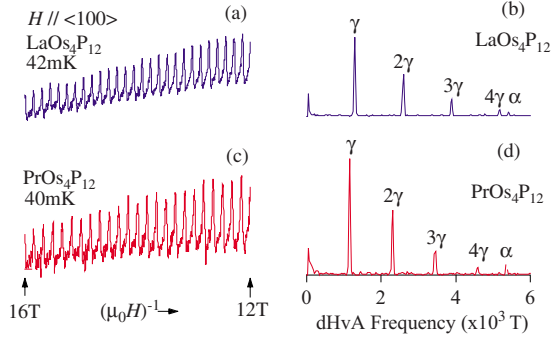


FIG. 1. (Color online) Comparison of [(a) and (c)] the typical dHvA oscillations and [(b) and (d)] the FFT spectra between $\text{LaOs}_4\text{P}_{12}$ and $\text{PrOs}_4\text{P}_{12}$.

in Ref. 14. The raw materials were 4*N* (99.99% pure) Pr, 3*N* La, 4*N* Os, 6*N* P, and 5*N* Sn. The crystal structures of filled skutterudite, belonging to the space group $Im\bar{3}$ (T_h^5 , No. 204) (Ref. 16) were verified by the powder x-ray-diffraction experiments. The residual resistivity ratios (RRRs) of the present samples are 180 for $\text{LaOs}_4\text{P}_{12}$ and 390 for $\text{PrOs}_4\text{P}_{12}$, respectively, indicating the high sample quality. The dHvA experiments were performed in a top loading dilution refrigerator cooled down to ~ 30 mK with a 17 T superconducting magnet. The dHvA signals were detected by means of the conventional field modulation method with a low frequency ($f \sim 10$ Hz).

III. RESULTS AND DISCUSSION

Figures 1(a) and 1(c) show typical recorder traces of the dHvA oscillations in $\text{LaOs}_4\text{P}_{12}$ and $\text{PrOs}_4\text{P}_{12}$ for the field H along $\langle 100 \rangle$ direction and Figs. 1(b) and 1(d) show their fast Fourier transformation (FFT) spectra. Two fundamental dHvA branches labeled α and γ have been observed in both compounds. The harmonics of γ branch are 2γ , 3γ , and 4γ . Figures 2(a) and 2(b) show the angular dependences of these dHvA branches. The largest frequency branches α were observed only in the limited angular ranges around $\langle 100 \rangle$ direction, which suggests the existence of multiply connected FS as shown later. The γ branches were observed over the whole field angles both in the (010) plane and the (110) plane with a slight angular dependence, indicating almost spherical FS. These angular dependences are close to each other between $\text{PrOs}_4\text{P}_{12}$ and $\text{LaOs}_4\text{P}_{12}$ except the slight difference of the magnitude in γ branch, indicating almost the same FS topology between these compounds and the localized nature of 4*f* electrons in $\text{PrOs}_4\text{P}_{12}$.

In order to assign the origin of dHvA branches, the band-structure calculations for $\text{LaOs}_4\text{P}_{12}$ and $\text{PrOs}_4\text{P}_{12}$ have been carried out based on the FLAPW method within the LDA. The details of the band-structure calculation have been reported elsewhere.⁹ The lattice constants and fractional coordinates of P at 24*g* site used in the band-structure calculations are $a = 8.0932$ Å and $(u, v) = (0.1434, 0.3576)$ for $\text{LaOs}_4\text{P}_{12}$ and $a = 8.080$ Å and $(u, v) = (0.14304, 0.35722)$ for $\text{PrOs}_4\text{P}_{12}$, respectively.^{14,17} The calculated band structure and density of states for $\text{LaOs}_4\text{P}_{12}$ are shown in Figs. 3(a) and

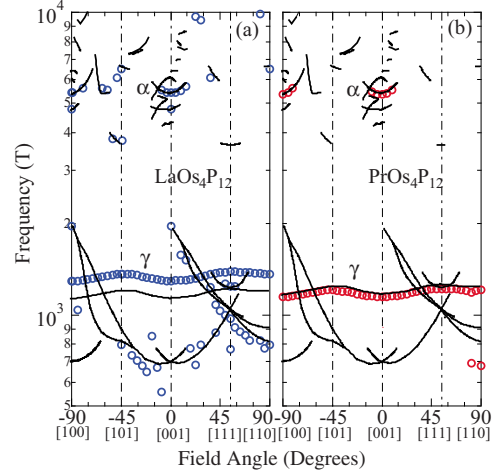


FIG. 2. (Color online) Comparison of the angular dependence of dHvA frequency between (a) $\text{LaOs}_4\text{P}_{12}$ and (b) $\text{PrOs}_4\text{P}_{12}$. Solid curves in both these figures are the results of band-structure calculations.

3(b), respectively. The 48th bands, which mainly consist of P 3*p* and Os 5*d* electrons, are located at the Fermi energy E_F with large density of states. The density of states at E_F is calculated as 86.76 states/Ry, which corresponds to the Sommerfeld coefficient of 15.04 mJ/K² mol. As shown in Figs.

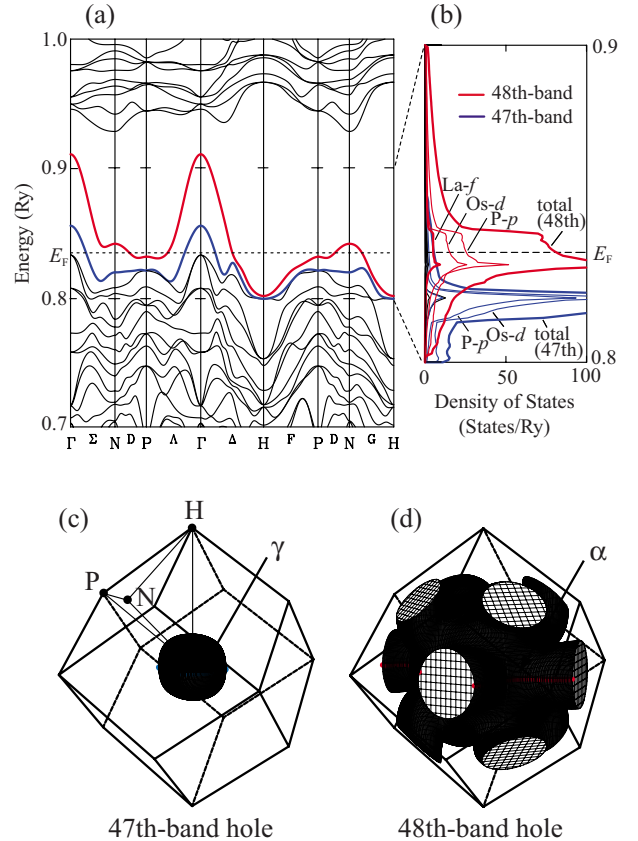


FIG. 3. (Color online) Band structure and Fermi surface of $\text{LaOs}_4\text{P}_{12}$. (a) is the energy-band structure, (b) is the partial and total density of states both of 47th and 48th bands, (c) and (d) are the 47th- and 48th-band hole Fermi surfaces, respectively.

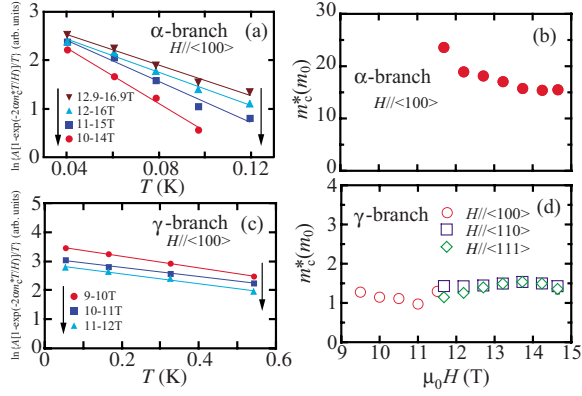


FIG. 4. (Color online) Temperature dependences of the dHvA amplitude at selected field ranges for (a) α branch and (c) γ branch for field along $H \parallel \langle 100 \rangle$ in $\text{PrOs}_4\text{P}_{12}$, and the corresponding field dependences of the cyclotron effective mass for (b) α branch and (d) γ branch.

3(c) and 3(d), the FS consists of two sheets; an almost spherical 47th-band hole sheet and a multiply connected 48th-band hole sheet. The results of band-structure calculation for $\text{PrOs}_4\text{P}_{12}$ (not shown) are almost the same with that of $\text{LaOs}_4\text{P}_{12}$.¹⁵ These FSs reasonably explain the observed dHvA frequency branches as shown in Figs. 2(a) and 2(b). It is obvious that the 48th-band FS has no proper nesting condition in contrast with the nice nesting condition in the corresponding FSs of $\text{PrFe}_4\text{P}_{12}$ and $\text{PrRu}_4\text{P}_{12}$.¹⁰ This fact confirms that the FS nesting with $q=(1,0,0)$ is crucial for the unusual phase transitions in $\text{PrFe}_4\text{P}_{12}$ and $\text{PrRu}_4\text{P}_{12}$.

As another piece of crucial information, we have estimated the cyclotron effective mass m_c^* from the temperature dependence of the dHvA amplitude, the so-called mass plot. The examples of the mass plot at the selected field ranges are shown in Figs. 4(a) and 4(c). The estimated m_c^* for α branch at the field between 10 and 16.9 T is $18m_0$ and m_c^* s for γ branch at the field between 9 and 12 T are ranging 1.2– $1.5m_0$ depending on the field directions. The dHvA frequency F and m_c^* for α and γ branches in $\text{PrOs}_4\text{P}_{12}$ are summarized in Table I comparing with those for $\text{LaOs}_4\text{P}_{12}$. For $\text{LaOs}_4\text{P}_{12}$, m_c^* s are relatively large as those for a La compound, roughly twice enhanced for each branch compared with the band-structure calculation. Such a large mass enhancement is a common feature in La skutterudites,^{9,11,18} which may originate from the electron-phonon interactions. In contrast, the observed effective mass $m_c^*=18m_0$ for α branch in $\text{PrOs}_4\text{P}_{12}$ is quite large as that for a Pr compound,

which is unusual taking into account the localized nature of $4f$ electrons and is difficult to be explained by the electron-phonon interaction. For the comparison with the mass enhancement estimated from the specific-heat measurements, we have estimated the Sommerfeld coefficients from the FS volumes and m_c^* in the present experiments assuming spherical FSs. The estimated values are $62 \text{ mJ/K}^2 \text{ mol}$ for $\text{PrOs}_4\text{P}_{12}$ and $18 \text{ mJ/K}^2 \text{ mol}$ for $\text{LaOs}_4\text{P}_{12}$, which are close to the results of specific-heat measurements by Matsuhira *et al.*¹³

It should be noted here that the mass enhancement compared to $\text{LaOs}_4\text{P}_{12}$ is branch dependent; 3.8 times for α branch and ~ 1.1 times for γ branch enhanced, respectively, which may originate from the difference of c - f interaction between the 48th and 47th bands in $\text{PrOs}_4\text{P}_{12}$. In fact, the present band-structure calculation for $\text{LaOs}_4\text{P}_{12}$ indicates the larger $4f$ component in the 48th band and the smaller one in 47th band at the Fermi energy as shown in Fig. 3(b), which suggests a stronger hybridization for 48th bands particularly in $\text{PrOs}_4\text{P}_{12}$ with $4f$ electrons. It should be also noted that m_c^* only for α branch in $\text{PrOs}_4\text{P}_{12}$ is suppressed by magnetic fields as shown in Fig. 4(b); it decreases $\sim 34\%$ with increasing magnetic fields from 11.7 to 14.6 T, whereas such a suppression has not been observed for γ branch within the present experimental magnetic field range as shown in Fig. 4(d).

Such a strong suppression of effective mass by the magnetic fields has been also observed in $\text{PrFe}_4\text{P}_{12}$.⁶ In $\text{PrFe}_4\text{P}_{12}$, an evident Kondo effect has been observed in the transport measurements; the temperature dependence of electrical resistivity ρ shows a $-\ln T$ dependence below ~ 100 K and exhibits a shallow peak at $T_P \sim 13$ K below which ρ shows a negative magnetoresistance,^{4,7} which may be an origin of the strong suppression of m_c^* at high fields. In contrast, the temperature dependence of ρ in $\text{PrOs}_4\text{P}_{12}$ shows ordinary metallic temperature dependence and only a small positive magnetoresistance up to 8 T below 30 K.¹⁴ Moreover, the specific heat below 10 K is insensitive to the magnetic fields up to 5 T.¹³ Thus the Kondo effect is not evident in $\text{PrOs}_4\text{P}_{12}$ except the present dHvA experiments at high fields.

Now let us consider the large mass enhancement in $\text{PrOs}_4\text{P}_{12}$ and why both $\text{PrFe}_4\text{P}_{12}$ and $\text{PrRu}_4\text{P}_{12}$ show the phase transition but $\text{PrOs}_4\text{P}_{12}$ does not. Since the low-lying crystalline electric field (CEF) level scheme is essential for the low-temperature physical properties, we compare the basic properties in Pr skutterudites, together with the low-lying CEF level schemes, as shown in Table II.^{2,5,13,19–28} Under the CEF of T_h symmetry in skutterudites, the $J=4$ multiplet of

TABLE I. Comparison of the dHvA frequency F and the cyclotron effective mass m_c^* between $\text{PrOs}_4\text{P}_{12}$ and $\text{LaOs}_4\text{P}_{12}$.

Field direction	Branch	$\text{PrOs}_4\text{P}_{12}$ (Expt.)		$\text{LaOs}_4\text{P}_{12}$ (Expt.)		$\text{PrOs}_4\text{P}_{12}$ (Theor.)		$\text{LaOs}_4\text{P}_{12}$ (Theor.)	
		F ($\times 10^3$ T)	m_c^* (m_0)	F ($\times 10^3$ T)	m_c^* (m_0)	F ($\times 10^3$ T)	m_c^* (m_0)	F ($\times 10^3$ T)	m_c^* (m_0)
$H \parallel \langle 100 \rangle$	α	5.36	18	5.42	4.7	5.387	1.956	5.366	1.957
	γ	1.15	1.2	1.29	1.1	1.167	0.561	1.134	0.557
$H \parallel \langle 110 \rangle$	γ	1.21	1.5	1.37	1.3	1.234	0.618	1.120	0.615
$H \parallel \langle 111 \rangle$	γ	1.22	1.3	1.39	1.2	1.252	0.628	1.121	0.627

TABLE II. Comparison of the basic properties in $\text{PrT}_4\text{X}_{12}$, the FS nesting with $q=(1,0,0)$ exists (\circ) or not (\times), lattice constant a , transition temperature T_{TR} to the ordered state (T_A : multipolar order; T_{MI} : metal-insulator transition; T_S : superconducting transition), Sommerfeld coefficients of Pr (γ_{Pr}) and La skutterudites (γ_{La}), CEF ground state (CEF-GS), the first excited state (CEF-first ES), and its excitation energy Δ_{first} . Note that the most possible CEF level schemes suggested by the inelastic neutron-scattering experiments are listed.

	$\text{PrFe}_4\text{P}_{12}$	$\text{PrRu}_4\text{P}_{12}$	$\text{PrOs}_4\text{P}_{12}$	$\text{PrRu}_4\text{Sb}_{12}$	$\text{PrOs}_4\text{Sb}_{12}$
FS nesting	\circ	\circ	\times	\times	\times
a (\AA)	7.813	8.042	8.080	9.265	9.303
T_{TR}	T_A	T_{MI}	No order	T_S	T_S
	6.5 K	63 K	>70 mK	1.3 K	1.85 K
γ_{Pr} ($\text{mJ}/\text{K}^2 \text{ mol}$)	1200–2700	<60	56.5	59	310–750
γ_{La} ($\text{mJ}/\text{K}^2 \text{ mol}$)	57	26	21.6	37	36
CEF-first ES	$\Gamma_4^{(1)}$	$\Gamma_4^{(1)}$	$\Gamma_4^{(2)}$	$\Gamma_4^{(2)}$	$\Gamma_4^{(2)}$
Δ_{first}	~ 22 K	68 K	46 K	65 K	~ 8 K
CEF-GS	Γ_1	Γ_1	Γ_1	Γ_1	Γ_1
References	5 and 19	20–22	13 and 23	24 and 25	26–28

Pr^{3+} ions splits into a singlet Γ_1 , a doublet Γ_{23} , and two triplets $\Gamma_4^{(1)}$ and $\Gamma_4^{(2)}$.²⁹ The triplets can be expressed as linear combinations of Γ_4 and Γ_5 for O_h symmetry, where $\Gamma_4^{(1)}$ is dominantly composed of Γ_4 having large dipole moment and $\Gamma_4^{(2)}$ is dominantly composed of Γ_5 having large quadrupole moment. In Table II, the most possible low-lying CEF level schemes, i.e., the ground state, first excited state, and its excitation energy Δ_{first} , suggested by the inelastic neutron-scattering (INS) experiments, are listed.

It is evident that the mass enhancement in the typical heavy-fermion compounds $\text{PrFe}_4\text{P}_{12}$ and $\text{PrOs}_4\text{Sb}_{12}$ is extremely large compared with other compounds, which may originate from the small CEF excitation energy Δ_{first} between the ground state and the first excited state; i.e., magnetic and/or multipole degree of freedom at the first excited states play the important role for the heavy-fermion behavior and also the unusual superconducting behavior. It is also evident that the mass enhancement in $\text{PrRu}_4\text{P}_{12}$ ($\gamma_{\text{Pr}}/\gamma_{\text{La}}=2.3$) and $\text{PrOs}_4\text{P}_{12}$ ($\gamma_{\text{Pr}}/\gamma_{\text{La}}=2.6$) is larger than that in $\text{PrRu}_4\text{Sb}_{12}$ ($\gamma_{\text{Pr}}/\gamma_{\text{La}}=1.6$). These compounds have relatively large Δ_{first} and the low-temperature properties are expected to be hardly affected by the first excited states. Nevertheless, in $\text{PrT}_4\text{P}_{12}$ with smaller lattice constant, the stronger c - f hybridization can be expected compared to $\text{PrT}_4\text{Sb}_{12}$ with larger lattice constant. In fact, the observed CEF excitation spectra of the INS experiments in $\text{PrFe}_4\text{P}_{12}$ and $\text{PrRu}_4\text{P}_{12}$ above the transition temperature are broader compared to that in $\text{PrT}_4\text{Sb}_{12}$ ($T=\text{Ru}$ or Os),^{19,22,25,27,28} which can be ascribed to the strong c - f hybridization. Therefore, the strong c - f interaction can be also expected for an origin of the large mass enhancement in $\text{PrOs}_4\text{P}_{12}$.

On the phase transitions in $\text{PrFe}_4\text{P}_{12}$ and $\text{PrRu}_4\text{P}_{12}$, the strong c - f interaction is also necessary to consider since La homolog without $4f$ electrons, which has basically the same FS topology, does not show the phase transition. The $4f$ electron's contribution based on the low-lying Γ_1 - $\Gamma_4^{(1)}$ CEF state, cooperating within the FS nesting may promote phase transitions in $\text{PrFe}_4\text{P}_{12}$ and $\text{PrRu}_4\text{P}_{12}$. Recently, from the theoretical point of view, the characteristics of hybridization and

multipole ordering of $4f$ electrons in Pr skutterudites were discussed in terms of the CEF energy-level schemes by Kuramoto and co-workers,^{30–32} where it has been proposed that the nature of first excited triplet state above the Γ_1 singlet ground state and the magnitude of Δ_{first} play an important role for unusual orderings both in $\text{PrFe}_4\text{P}_{12}$ and $\text{PrRu}_4\text{P}_{12}$ and also for the heavy-fermion state in $\text{PrFe}_4\text{P}_{12}$. In their theory, the heavy fermion and strongly hybridized state in $\text{PrFe}_4\text{P}_{12}$ are attributed to the Kondo effect within the quartet Γ_1 - $\Gamma_4^{(1)}$ CEF level scheme. The difference of the CEF state and/or the strength of c - f interaction may be the origin of diversity of the ground state in Pr-based skutterudites.

Finally we give a comment on a comparison between the physical properties of $\text{PrOs}_4\text{P}_{12}$ and those of $\text{PrRu}_4\text{Sb}_{12}$ and $\text{PrOs}_4\text{Sb}_{12}$, since the latter two compounds have also no nesting property in FS and are believed to have a similar CEF level scheme with that of $\text{PrOs}_4\text{P}_{12}$. This comparison may be more informative to understand the heavy-fermion state in $\text{PrOs}_4\text{P}_{12}$. $\text{PrOs}_4\text{P}_{12}$ and $\text{PrOs}_4\text{Sb}_{12}$ are most likely to be a heavy-fermion system, however, $\text{PrRu}_4\text{Sb}_{12}$ seems to be a normal metal, judging from the cyclotron effective mass determined by the dHvA experiments.³³ The superconductivity in $\text{PrRu}_4\text{Sb}_{12}$ is also conventional BCS type,^{24,34,35} which is in contrast with the unconventional one in $\text{PrOs}_4\text{Sb}_{12}$.³⁶ On the other hand, it is interesting why only $\text{PrOs}_4\text{P}_{12}$ shows no superconductivity though the ground state is nonmagnetic. The large mass enhancement and field-induced quadrupolar ordering at low temperatures in $\text{PrOs}_4\text{Sb}_{12}$ were explained by the low-lying Γ_1 - $\Gamma_4^{(2)}$ CEF state with a small value of $\Delta_{\text{first}} \sim 8$ K, namely, the almost degenerated quartet of the CEF state give rise to the large mass enhancement and its level crossing with increasing magnetic field causes the field-induced quadrupolar ordering.^{37,38} On the other hand, $\text{PrOs}_4\text{P}_{12}$ and $\text{PrRu}_4\text{Sb}_{12}$ have relatively larger Δ_{first} , although the Δ_{first} of $\text{PrOs}_4\text{P}_{12}$ is about 30% smaller than that of $\text{PrRu}_4\text{Sb}_{12}$. The smaller Δ_{first} and the stronger c - f interaction may cause the heavy-fermion behavior in $\text{PrOs}_4\text{P}_{12}$. However, further elaborated investigations, such as the magnetization and the specific-heat measurements at higher fields,

are necessary to confirm the relation between the CEF state and the heavy-fermion behavior.

IV. SUMMARY

We have measured the dHvA effect in $\text{PrOs}_4\text{P}_{12}$ and its reference compound $\text{LaOs}_4\text{P}_{12}$. Multiply connected and almost spherical FSs, whose cyclotron effective masses are highly enhanced up to $18m_0$, have been observed. We have confirmed that the FS topology in $\text{PrOs}_4\text{P}_{12}$ has no nesting property of $q=(1,0,0)$, which is in large contrast to those of $\text{PrFe}_4\text{P}_{12}$ and $\text{PrRu}_4\text{P}_{12}$. The strong c - f interaction may be

necessary for the phase transitions in $\text{PrFe}_4\text{P}_{12}$ and $\text{PrRu}_4\text{P}_{12}$, in addition to the nesting properties of FS.

ACKNOWLEDGMENTS

We would like to thank K. Iwasa for informative discussion. This work was supported by a Grant-in-Aid for Scientific Research Priority Area Skutterudite (Contracts No. 15072204 and No. 15072206), New Materials Science Using Regulated Nano Spaces (No. 20045008-01), and Scientific Research (C) (No. 20540358) of the Ministry of Education, Culture, Sports, Science, and Technology of Japan.

- ¹Y. Aoki, H. Sugawara, H. Harima, and H. Sato, *J. Phys. Soc. Jpn.* **74**, 209 (2005).
- ²H. Sato, D. Kikuchi, K. Tanaka, H. Aoki, K. Kuwahara, Y. Aoki, M. Kohgi, H. Sugawara, and K. Iwasa, *J. Magn. Magn. Mater.* **310**, 188 (2007).
- ³M. B. Maple, Z. Henkie, W. M. Yuhasz, P.-C. Ho, T. Yanagisawa, T. A. Sayles, N. P. Butch, J. R. Jeffries, and A. Pietraszko, *J. Magn. Magn. Mater.* **310**, 182 (2007).
- ⁴H. Sato, Y. Abe, H. Okada, T. D. Matsuda, K. Abe, H. Sugawara, and Y. Aoki, *Phys. Rev. B* **62**, 15125 (2000).
- ⁵Y. Aoki, T. Namiki, T. D. Matsuda, K. Abe, H. Sugawara, and H. Sato, *Phys. Rev. B* **65**, 064446 (2002).
- ⁶H. Sugawara, T. D. Matsuda, K. Abe, Y. Aoki, H. Sato, S. Nojiri, Y. Inada, R. Settai, and Y. Ōnuki, *Phys. Rev. B* **66**, 134411 (2002).
- ⁷H. Sugawara, A. Kuramochi, T. Namiki, T. D. Matsuda, Y. Aoki, and H. Sato, *J. Phys. Soc. Jpn.* **77**, 085001 (2008).
- ⁸C. Sekine, T. Uchiyumi, I. Shirotnani, and T. Yagi, *Phys. Rev. Lett.* **79**, 3218 (1997).
- ⁹H. Sugawara, Y. Abe, Y. Aoki, H. Sato, M. Hedo, R. Settai, Y. Ōnuki, and H. Harima, *J. Phys. Soc. Jpn.* **69**, 2938 (2000).
- ¹⁰H. Harima and K. Takegahara, *Physica B* **312-313**, 843 (2002).
- ¹¹S. R. Saha, H. Sugawara, Y. Aoki, H. Sato, Y. Inada, H. Shishido, R. Settai, Y. Ōnuki, and H. Harima, *Phys. Rev. B* **71**, 132502 (2005).
- ¹²H. Harima, *J. Phys. Soc. Jpn.* **77**, Suppl. A, 114 (2008).
- ¹³K. Matsuhira, Y. Doi, M. Wakeshima, Y. Hinatsu, K. Kihou, C. Sekine, and I. Shirotnani, *Physica B* **359-361**, 977 (2005).
- ¹⁴M. W. Yuhasz, P.-C. Ho, T. A. Sayles, T. Yanagisawa, N. A. Frederick, M. B. Maple, P. Rogl, and G. Giester, *J. Phys.: Condens. Matter* **19**, 076212 (2007).
- ¹⁵H. Sugawara *et al.*, *J. Phys. Soc. Jpn.* **77**, Suppl. A, 108 (2008).
- ¹⁶W. Jeitschko and D. Braun, *Acta Crystallogr., Sect. B: Struct. Crystallogr. Cryst. Chem.* **33**, 3401 (1977).
- ¹⁷Y. Iwahashi, H. Sugawara, K. Magishi, T. Saito, K. Koyama, R. Settai, Y. Ōnuki, G. Giester, and P. Rogl, *J. Phys. Soc. Jpn.* **77**, Suppl. A, 219 (2008).
- ¹⁸H. Sugawara, S. Osaki, S. R. Saha, Y. Aoki, H. Sato, Y. Inada, H. Shishido, R. Settai, Y. Ōnuki, H. Harima, and K. Oikawa, *Phys. Rev. B* **66**, 220504(R) (2002).
- ¹⁹K. Iwasa, L. Hao, T. Hasegawa, K. Horiuchi, Y. Murakami, J. Otsuki, Y. Kuramoto, M. Kohgi, K. Kuwahara, H. Sugawara, Y. Aoki, and H. Sato, *J. Phys. Soc. Jpn.* **77**, 063706 (2008).
- ²⁰C. Sekine, T. Inaba, I. Shirotnani, M. Yokoyama, H. Amitsuka, and T. Sakakibara, *Physica B* **281-282**, 303 (2000).
- ²¹K. Matsuhira, Y. Hinatsu, C. Sekine, and I. Shirotnani, *Physica B* **312-313**, 829 (2002).
- ²²K. Iwasa, L. Hao, K. Kuwahara, M. Kohgi, S. R. Saha, H. Sugawara, Y. Aoki, H. Sato, T. Tayama, and T. Sakakibara, *Phys. Rev. B* **72**, 024414 (2005).
- ²³K. Iwasa, K. Saito, Y. Murakami, and H. Sugawara (unpublished). Recently, they performed the inelastic neutron-scattering experiments and determined the CEF level scheme in $\text{PrOs}_4\text{P}_{12}$. The result is consistent with the previous works (Refs. 13 and 14).
- ²⁴N. Takeda and M. Ishikawa, *J. Phys. Soc. Jpn.* **69**, 868 (2000).
- ²⁵D. T. Adroja, J.-G. Park, E. A. Goremychkin, N. Takeda, M. Ishikawa, K. A. McEwen, R. Osborn, A. D. Hillier, and B. D. Rainford, *Physica B* **359-361**, 983 (2005).
- ²⁶E. D. Bauer, N. A. Frederick, P.-C. Ho, V. S. Zapf, and M. B. Maple, *Phys. Rev. B* **65**, 100506(R) (2002).
- ²⁷K. Kuwahara, K. Iwasa, M. Kohgi, K. Kaneko, S. Araki, N. Metoki, H. Sugawara, Y. Aoki, and H. Sato, *J. Phys. Soc. Jpn.* **73**, 1438 (2004).
- ²⁸E. A. Goremychkin, R. Osborn, E. D. Bauer, M. B. Maple, N. A. Frederick, W. M. Yuhasz, F. M. Woodward, and J. W. Lynn, *Phys. Rev. Lett.* **93**, 157003 (2004).
- ²⁹K. Takegahara, H. Harima, and A. Yanase, *J. Phys. Soc. Jpn.* **71**, 372 (2002).
- ³⁰Y. Kuramoto, A. Kiss, J. Otsuki, and H. Kusunose, *J. Phys. Soc. Jpn.* **75**, Suppl., 209 (2006).
- ³¹A. Kiss and Y. Kuramoto, *J. Phys. Soc. Jpn.* **74**, 2530 (2005).
- ³²J. Otsuki, H. Kusunose, and Y. Kuramoto, *J. Phys. Soc. Jpn.* **74**, 200 (2005).
- ³³T. D. Matsuda, K. Abe, F. Watanuki, H. Sugawara, Y. Aoki, H. Sato, Y. Inada, R. Settai, and Y. Ōnuki, *Physica B* **312-313**, 832 (2002).
- ³⁴M. Yogi, H. Kotegawa, Y. Imamura, G.-q. Zheng, Y. Kitaoka, H. Sugawara, and H. Sato, *Phys. Rev. B* **67**, 180501(R) (2003).
- ³⁵E. E. M. Chia, M. B. Salamon, H. Sugawara, and H. Sato, *Phys. Rev. B* **69**, 180509(R) (2004).
- ³⁶Y. Aoki, T. Tayama, T. Sakakibara, K. Kuwahara, K. Iwasa, M. Kohgi, W. Higemoto, D. E. MacLaughlin, H. Sugawara, and H. Sato, *J. Phys. Soc. Jpn.* **76**, 051006 (2007).
- ³⁷T. Tayama, T. Sakakibara, H. Sugawara, Y. Aoki, and H. Sato, *J. Phys. Soc. Jpn.* **72**, 1516 (2003).
- ³⁸M. Kohgi, K. Iwasa, M. Nakajima, N. Metoki, S. Araki, N. Bernhoeft, J. M. Mignot, A. Gukasov, H. Sato, Y. Aoki, and H. Sugawara, *J. Phys. Soc. Jpn.* **72**, 1002 (2003).